Shape-Based Image Retrieval Using Pair-Wise Candidate Co-ranking

A. El-ghazal[1], O. Basir[1], and S. Belkasim[2]

[1] Electrical and Computer Engineering, University of Waterloo, ON., Canada
[2] Computer Science, Georgia State University, Atlanta, GA., USA

Abstract. Shape-based image retrieval is one of the most challenging aspects in Content-Based Image Retrieval (CBIR). A variety of techniques are reported in the literature that aim to retrieve objects based on their shapes; each of these techniques has its advantages and disadvantages. In this paper, we propose a novel scheme that exploits complementary benefits of several shape-based image retrieval techniques and integrates their assessments based on a pair-wise co-ranking process. The proposed scheme can handle any number of CBIR techniques; however, three common techniques are used in this study: Invariant Zernike Moments (IZM), Multi-Triangular Area Representation (MTAR), and Fourier Descriptor (FD). The performance of the proposed scheme is compared with that of each of the selected techniques. As will be demonstrated in this paper, the proposed co-ranking scheme exhibits superior performance.

Keywords: Co-ranking, Image retrieval, Shape.

1 Introduction

Recent years have witnessed increased interest in digital imaging. The ease and convenience of capturing, transmitting, and storing digital images in personal and public image databases are considered contributing factors behind this increased interest. The internet is already rich in image depositories that cover a wide range of applications, including, biomedical, multimedia, geological, and astronomy. Although, the storage format of image data is relatively standardized, the retrieval process of images from an image depository tends to be quite complex, and thus it has become a limiting factor that needs to be addressed.

Typically, images in a database are retrieved based on either textual information or content information. Early retrieval techniques were based on textual annotation of images. Images were first annotated with text and then searched based on their textual tags. However, text-based techniques have many limitations, including their reliance on manual annotation, which can be a difficult and tedious process for large image sets. Furthermore, the rich content typically found in images and the subjectivity of the human perception make the task of describing images using words a difficult if not an impossible task.

To overcome these difficulties, Content Based Image Retrieval (CBIR) was proposed [1]. This approach relies on the visual content of images, rather than textual annotations, to search for images; and hence, has the potential to be more effective in

M. Kamel and A. Campilho (Eds.): ICIAR 2007, LNCS 4633, pp. 650–661, 2007.

responding to more specific user queries. CBIR techniques use visual contents such as color, texture, and shape to represent and index the image. Visual contents such as color and texture have been explored more thoroughly than shape contents .The increasing interest in using the shape features of objects for CBIR is not surprising, given the considerable evidence that natural objects are recognized primarily by their shape [2, 3]. A survey of users on the cognition aspects of image retrieval confirmed that users prefer retrieving images based on shape to color and texture [4]. However, retrieval based on shape content remains more difficult compared to image retrieval based on other visual features [2].

During the last decade, significant progress has been made in both the theoretical and practical research aspects of shape-based image retrieval [5, 6]. Shape representation approaches can be divided into two main categories, namely: region-based approaches and boundary-based approaches (also known as contour-based approaches). Region-based approaches often use moment descriptors to describe shapes. These descriptors include geometrical moments [7], Zernike moments [8, 9], pseudo-Zernike moments [10], and Legendre moments [8]. Although region-based approaches are global in nature and can be applied to generic shapes, they fail to distinguish between similar objects [11]. In many applications, the internal content of the shape is not as important as its boundary. Boundary-based techniques tend to be more efficient for handling shapes that are describable by their object contours [11]. Many boundary-based techniques have been proposed in the literature, including Fourier descriptors [12], Curvature Scale Space (CSS) [13], wavelet descriptors [14], and contour displacement [15].

Though the number of available shape-based image retrieval techniques has been increasing rapidly such techniques still exhibit shortcomings. Techniques that have demonstrated reasonable robustness often tend to be computationally complex [15]. In this paper, we propose to integrate several of the existing in a pair-wise co-ranking scheme so as to obtain superior shape-based image retrieval performance.

The remaining of the paper is organized as follows: Section 2 introduces the problem formulation; while Section 3 discusses the proposed pair-wise co-ranking scheme. The process of formulating the final ranking decision of the group is presented in Section 4. Section 5 describes experiments to evaluate the performance of the proposed shape retrieval scheme. Conclusions from this study and suggestions for future work are presented in Section 6.

2 Problem Formulation

We consider a group of Image Retrieval techniques with complementary image representation capabilities. These techniques are viewed as agents cooperating to determine the best candidate image x from an ensemble of images Θ that matches a query image. This group of image retrieval agents is indexed by the set IRA = $\{IRA_1, IRA2,\ldots IRA_M\}$. Each agent IRA_i uses a feature extraction scheme F_i and a matching strategy Γ_i to determine a similarity measure S_i between query image x and all images $y \in \Theta$; that is,

$$S_i(x, y) = \Gamma_i(F_i(y), F_i(x)), \forall y \in \Theta \tag{1}$$

Each agent IRA_i establishes a ranking $R_i(y \mid F_i(y)) \in \{1,2,...N\}, \forall y \in \Theta$ such that $R_i(y \mid F_i(y)) \le R_j(z \mid F_j(z))$ implies $S_i(x,y) \ge S_j(x,z)$.

Without loss of generality, $R_i(y \mid F_i(y))$ can be viewed as an index set from 1 to N, where index 1, for example, points to the closest candidate image to the query image x, and index N points to the most dissimilar candidate image to the query image x. In general, index l in this set points to the image that is preceded by l-1 candidates; these candidates are viewed by IRA_i as better candidates for the query image x, than the candidate give the rank l. Since each agent uses a different feature extraction scheme, it is expected that the agents reach different ranking decisions for the different images in the set. Each of the CBIR techniques must demonstrate reasonable performance before it is selected to be a member of the group. It is thus reasonable to expect that good image candidates will cluster at the top of the ranking for all agents.

3 Pair-Wise Co-ranking Scheme

In the following discussion, we propose an information exchange scheme between the image retrieval agents so as to assist each in determining the best image as a candidate matching the user query. This scheme allows for exploiting the relative advantages and disadvantages of each agent.

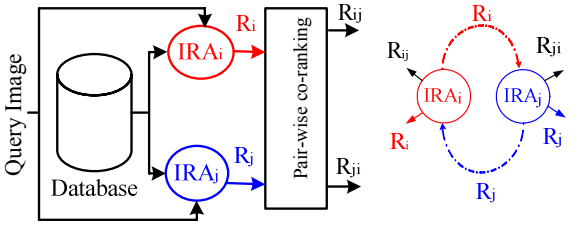

Fig. 1. Information exchange between two image retrieval agents regarding the ranking

Pair-wise co-ranking revolves around the hypothesis that each agent IRA_j may readjust its ranking of a candidate image if it is exposed to the ranking of another agent IRA_i. The communication process between two agents is depicted in Fig 1. The initial ranking of an agent is referred to as marginal ranking. This ranking reflects the assessment of the agent of closeness of each image to the query image. On the other hand, the revised ranking of an agent is referred to as conditional ranking. This ranking reflects how the assessment of an agent is influenced by other agents.

To set up the process of information exchange among the agents, the ranking set of each agent IRA_i is divided into two partitions: an Elite Candidates Partition (ECP_i) and a Potential Candidates Partition (PCP_i). It is expected that good matches to the query will cluster in the elite partitions. ECP contains the first m candidates; PCP contains the last N-m candidates. Thus, the marginal ranking of agent IRA_i can be viewed as a concatenation of two ranking sets; that is, $\mathrm{R}_i = \{R_i^{ECP}, R_i^{PCP}\}$. Where R_i^{ECP} is the ranking for $\mathbf{R}_i \le m$, and R_i^{PCP} is the ranking for $\mathbf{R}_i > m$.

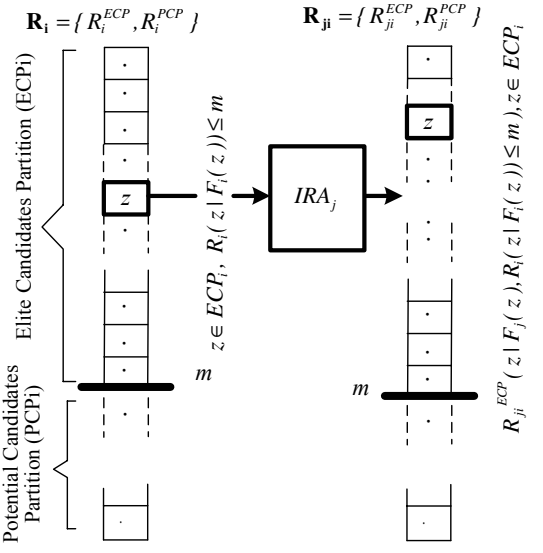

Fig. 2. Illustration of the pair-wise co-ranking scheme

We need to introduce the conditional ranking like what we did with the marginal. Then we show the example. Fig 2. depicts the process of forming conditional elites, where agent IRA_j revises its conditional elite partition ranking R_{ji}^{ECP}, based on the marginal ranking information provided by agent IRA_i. Here, image z is seen as an elite image by agent IRA_i. Agent IRA_j uses its own feature extraction scheme F_j to determine the rank of image z in its conditional elite candidates partition; that is,

$$R_{ji}^{ECP}(z \mid F_j(z), R_i(z \mid F_i(z)) \le m), z \in ECP_i \tag{2}$$

This formula can be read as follows: agent j re-ranks image z based on its feature extraction scheme $F_j(z)$, given that image z has been ranked as an elite candidate by agent IRA_i, based on the feature extraction scheme $F_i(z)$.

The fact that image z is placed in the conditional elite partition of agent IRA_j does not necessarily imply that image z is in the marginal elite partition of IRA_j. Similarly, the conditional ranking of the potential candidates partitions are computed,

$$R_{ji}^{PCP}(z \mid F_j(z), R_i(z \mid F_i(z)) > m), z \in PCP_i \tag{3}$$

The conditional ranking of agent IRA_j, based on information received from agent IRA_i is viewed as a concatenation of two ranking sets; that is,

$$\mathrm{R_{ji}} = \{R_{ji}^{ECP}, R_{ji}^{PCP}\} \tag{4}$$

The results of the above process are summarized in Table 1.

Table 1. Marginal and Pair-wise Conditional Rankings

$R_i^{ECP}(z\|F_i(z))\} \forall R_i \le m$ $R_i^{PCP}(z\|F_i(z))\} \forall R_i > m$, $\mathbf{R_i} = \{ R_i^{ECP}, R_i^{PCP} \}$ $R_{ij}^{ECP}(y\|F_i(z), R_j(y\|F_j(z)) \le m)\} \forall R_{ij} < m$ $R_{ij}^{PCP}(y\|F_i(z), R_j(y\|F_j(z)) > m)\} \forall R_{ij} > m$, $\mathbf{R_{ij}} = \{ R_{ij}^{ECP}, R_{ij}^{PCP} \}$
$R_j^{ECP}(z\|F_j(z))\} \forall R_j \le m$ $R_j^{PCP}(z\|F_j(z))\} \forall R_j > m$, $\mathbf{R_j} = \{ R_j^{ECP}, R_j^{PCP} \}$ $R_{ji}^{ECP}(y\|F_j(z), R_i(y\|F_i(z)) \le m)\} \forall R_{ji} \le m$ $R_{ji}^{PCP}(y\|F_j(z), R_i(y\|F_i(z)) > m)\} \forall R_{ji} > m$, $\mathbf{R_{ji}} = \{ R_{ji}^{ECP}, R_{ji}^{PCP} \}$

Example

The database, described in Section 5, consists of 70 classes, each class having 20 objects. The target is to see the relevant images ranked as the top twenty positions. Fig. 3 and 4 display the results produced by agents IRA_1 and IRA_2, respectively.

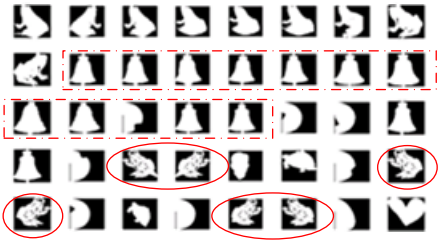

Fig. 3. Retrieved results of IRA_1 ($\mathbf{R_1}$)

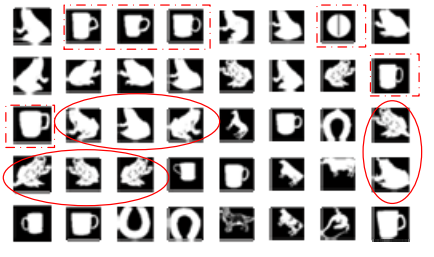

Fig. 4. Retrieved results of IRA_2 ($\mathbf{R_2}$)

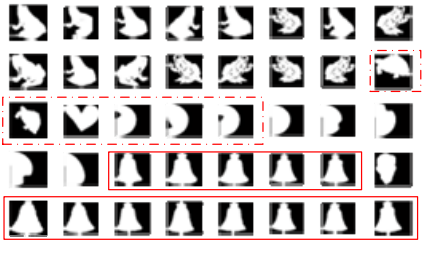

Fig. 5. Pair-wise conditional ranking of IRA_1 based on IRA_2 ($\mathbf{R_{21}}$)

In both figures the top left shape is the query shape (Frog); the retrieved shapes are arranged in descending order according to each shape's similarity to the query shape.

Fig. 3 indicates that the first agent IRA_1 has managed to correctly rank 9 of 20 shapes (45%). Furthermore, most of the irrelevant shapes, indicated by the dashed frame, are objects that belong to the same class (Bell). In Fig. 4, it is evident that the irrelevant shapes of agent IRA_2, indicated by the dashed frame, differ from those of agent IRA_1. Fig. 5 exhibits the conditional ranking of agent IRA_1 based on the ranking information it receives from the second agent IRA_2. Referring to Fig. 5, the irrelevant shapes of the first agent, indicated by the dashed frame in Fig. 3, do not appear at top-rank positions. The positions of the relevant shapes, encircled by the ellipses in Fig. 3, produced by the first agent IRA_1, are repositioned to the top 20 positions in $\mathbf{R_{21}}$, resulting in an accuracy of 75% (15 out of 20). It is clear that the pair-wise conditional ranking $\mathbf{R_{21}}$ is much better than the marginal rankings $\mathbf{R_1}$ and $\mathbf{R_2}$.

4 Reaching Decision

The main motivation behind this research work is to identify image retrieval techniques that capture different characteristics of an image and combine them so as to achieve an enhanced retrieval performance. These techniques are considered as a team of agents who cooperate to determine the best image in the database that matches the query image. This collaboration is accomplished via exchanging candidate ranking information. . Each agent uses its feature extraction scheme to compute a ranking $\mathbf{R_{ii}}$ (double indexing is used to simplify the mathematical notations) that reflects the technique's preference on the best candidate to match the query image (i.e., marginal ranking). . Furthermore, each agent is exposed to the ranking information of other agents so as to compute a conditional ranking of for each candidate image, as explained above. Therefore, M retrieval agents yield M^2 rankings: M marginal rankings, plus $M(M-1)$ conditional rankings. Fig. 6 depicts the ranking set of a three-agent system.

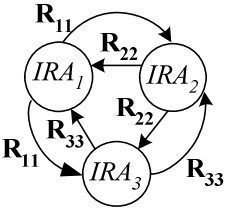

Fig. 6. Information exchange on the ranking of three image retrieval agents

For M agents, the ranking sets can be organized in a matrix format:

$$R = \begin{bmatrix} R_{11} & R_{12} \ldots\ldots & R_{1M} \\ R_{21} & R_{22} \ldots\ldots & R_{2M} \\ . & & . \\ . & & . \\ . & & . \\ R_{M1} & R_{M2} \ldots\ldots & R_{MM} \end{bmatrix}$$

Where $\mathbf{R_{ij}}$ is the conditional ranking of the i^{th} agent, given that the ranking of the j^{th} agent, and $\mathbf{R_{ii}}$ is the marginal ranking of the i^{th} agent.

Fig. 7 portrays rank information exchange that yields the group's rank decision on all candidates.

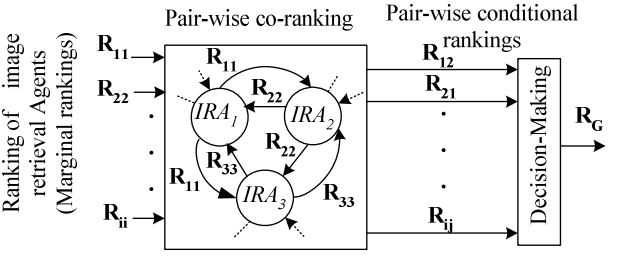

Fig. 7. Steps of applying the pair-wise co-ranking

The group rank of image z is defined as:

$$Score(z)=\sum_{\substack{i=1\\ i\neq j}}^{M}\sum_{\substack{j=1\\ i\neq j}}^{M}\mathrm{R}_{ij}(z\,|\,F_i(z),\mathrm{R}_j(z\,|\,F_j(z)) \tag{5}$$

The ranking scheme of all candidates is defined as

$$\mathrm{R}_G = sort(score(z))\forall z\in\Theta \tag{6}$$

Example

Fig. 8 displays the results produced by agent IRA_3 for the same query, the frog. As seen in this figure, agent IRA_3 has managed to rank 12 of the 20 shapes correctly (60%). Furthermore, one can notice that the images, indicated by the dashed frame at the top 20 positions, are identified by the other two agents IRA_1 and IRA_2 as being irrelevant. Thus, the conditional ranking of IRA_1, based on ranking information it has received from IRA_3, enables this agent to revise its assessment of relevance of the candidates. The relevant images, encircled by ellipses and produced by IRA_1, have moved to the top rank positions in R_{31}, resulting in an accuracy of 75% (15 out of 20), as illustrated in Fig. 9. After each agent revises its results, based on the ranking information it receives from the other two agents, a group ranking $\mathbf{R_G}$ of all pair-wise conditional rankings is obtained by using the formulation given by Equation (6). Fig. 10 exhibits the final ranking of the proposed pair-wise co-ranking scheme. This figure makes it clear that the exchange of ranking information enables the three agents to converge to better ranking decisions (an accuracy of 90%) than those of any individual agent; IRA_1, IRA_2 and IRA_3 achieving an accuracy of 45%, 70%, and 60%, respectively.

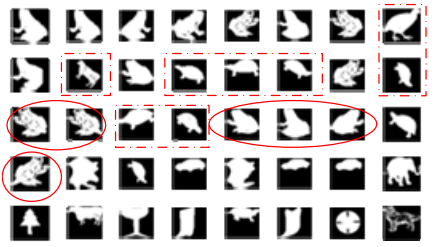

Fig. 8. Retrieved results of IRA_3 ($\mathbf{R_{33}}$)

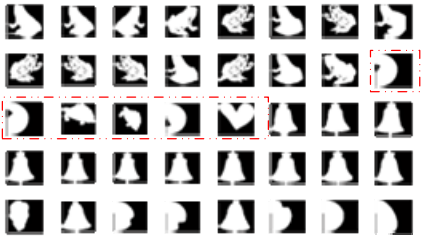

Fig. 9. Pair-wise conditional ranking of IRA_1 based on IRA_3 ($\mathbf{R_{31}}$)

Fig. 10. The final raking of the pair-wise co-ranking scheme $\mathbf{R_G}$

5 Experimental Results

We recognize the lack of a standard database to evaluate the different shape-based image retrieval techniques. Researchers in this field tend to develop their own databases, which are often limited in size and/or application scope. The MPEG-7 developers have built a database of a reasonable size and generality [11]. This database consists of three main sets: set A, set B, and set C. Set A consists of two subsets A_1 and A_2, and each subset includes 420 images. A_1 is used for testing scale invariance; set A_2 is used to test for rotation invariance. Set B consists of 1400 images that are classified into 70 classes, each class having 20 images. Set B is used to test for similarity-based retrieval performance, and to test the shape descriptors for robustness to various arbitrary shape distortions including rotation, scaling, arbitrary skew, stretching, defection, and indentation. For these reasons, set B is selected to evaluate the performance of the proposed pair-wise co-ranking scheme. Set C consists

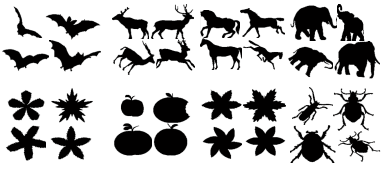

Fig. 11. Samples from set B of the MPEG-7 database

of 200 affine transformed Bream fish and 1100 marine fish that are unclassified. The 200 bream fish are designated as queries. This set is used to test the shape descriptors for robustness to non-rigid object distortions. Samples of the images from this database are depicted in Fig. 11.

To evaluate the image retrieval performance of the different techniques, a performance measure is required. Precision and recall are the most commonly used measures. Precision measures the retrieval accuracy, whereas recall measures the capability to retrieve relevant items from the database [16].

To evaluate the performance of the proposed pair-wise co-ranking scheme, experiments are conducted by using set B of the MPEG-7 database. All the contours of the images are resampled so that each contour consists of 128 points.

To implement and test the newly developed scheme, three techniques are selected.

The first technique is the Invariant Zernike Moment (IZM) method [9], a region-based technique that provides the global characteristics of an image. Zernike moments are effective both for image representation and as a global shape descriptor [17]. This technique is adopted by MPEG-7 as a standard region technique.

Multi-Triangular Area Representation (MTAR) is the second technique[18]. It is a boundary-based technique used to provide the local characteristics of an image for the proposed co-ranking scheme. The technique is designed such that it captures the local information using the triangular area. El-Rube et al. [18] have demonstrated that the MTAR technique outperforms the curvature scale space (CSS) technique, which is adopted by MPEG-7 as a standard boundary technique, in terms of accuracy. Moreover, the number of iterations of the MTAR image is limited to n/2+1, where n is the number of boundary points of an image, whereas the number of the iterations of the CSS image is not limited to a certain number. This renders the representation of the MTAR faster than that of the CSS.

The third technique is the Fourier Descriptor method, based on the Centroid Distance (CD) signature. According to Zhang [16], the Centroid Distance (CD) signature outperforms the Complex Coordinate (CC), Triangular Centroid Area (TCA) and the Chord-Length Distance (CLD) signatures. The reason for selecting the FD is that it is a boundary-based technique and can capture both local and global characteristics. The low frequency provides the global characteristics, and the high frequency symbolizes the local characteristics of an image[16].

To fuse the three techniques, the first 50 (m=50) retrieved results of each technique are considered an elite candidate partition in the revision stage.

Two experiments are conducted to evaluate the performance of the new co-ranking scheme. In the first experiment, the group-ranking scheme is compared with that of each technique. The precision-recall curves of the proposed approach and that of each of the three techniques are shown in Fig. 12. The precision value at a certain recall is the average of the precision values of all the database shapes at that recall.

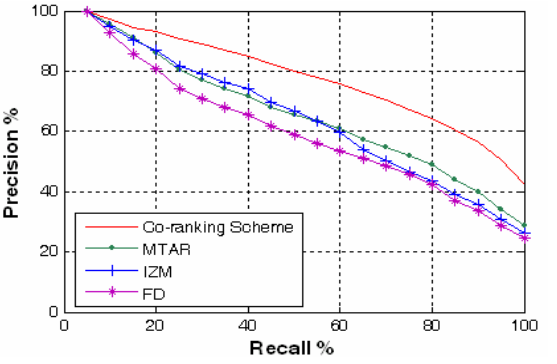

Fig. 12. Precision-recall curves of the proposed pair-wise co-ranking scheme, IZM, FD, and MTAR techniques

The precision-recall curves in Fig. 12 show that the proposed approach outperforms each of the three techniques: the IZM, FD, and MTAR techniques.

In the second experiment, we compare the relative performance of the proposed co-ranking scheme under two conditions: 1) Group ranking based on pooling the pair-wise conditional rankings of individual techniques. 2) Group ranking based on pooling the marginal rankings of the individual techniques. As can be seen in Fig. 13, there are six pair-wise conditional rankings (R_{ij}, $i \neq j$, i,j=1,2,3), and three marginal rankings (R_{ij}, i=j, i=1,2,3).Fig. 14 depicts the precision-recall curves for the pooling of the pair-wise conditional rankings and pooling the marginal rankings. It is evident from this figure how the performance of the pair-wise co-ranking scheme is superior to that of pooling only the marginal rankings. This demonstrates the value of communication among the three techniques in selecting the best match to the query image.

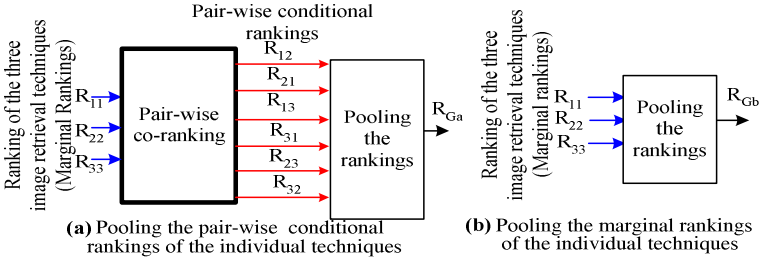

Fig. 13. Pooling the pair-wise conditional rankings and pooling the marginal rankings of the individual techniques

Table 2 summarizes the average accuracy of relevance of the closest shapes retrieved from 1400-image database for: IZM, FD, MTAR, pooled marginal rankings, and pair-wise conditional co-ranking.

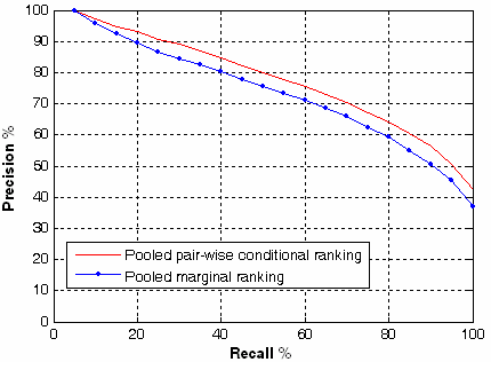

Fig. 14. Precision-recall curves of the pair-wise co-ranking and the pooled marginal ranking

Table 2. Retrieval performance of the IZM,FD, MTAR,pooled marginal ranking, and the pooled pair-wise conditional ranking

Method	IZM	FD	MTAR	Pooled marginal ranking	pair-wise conditional co-ranking
Accuracy%	59.16	54.61	60.01	67.32	71.35

It clear from Table 2 that the pair-wise conditional co-ranking scheme (with accuracy of 71.35%) outperformed the pooling of the marginal rankings (with accuracy of 67.32%) as well as IZM (with accuracy of 59.16%), FD (with accuracy of 54.61%), and MTAR (with accuracy of 60.01%).

6 Conclusions

This paper presents a new pair-wise co-ranking scheme that aims to improve the retrieval performance by combining the ranking decisions of a group of shape-based image retrieval techniques. Experimental results are presented to investigate the performance of the proposed scheme using set B of the widely used MPEG-7 database.

The experimental results demonstrate that the proposed pair-wise co-ranking scheme yields better results than those of each of the three selected techniques.

Furthermore, the performance of the proposed co-ranking scheme is superior to that of pooling the three individual rankings. This improvement is accomplished by allowing the individual retrieval techniques to exchange their ranking information in a pair-wise manner. The overall reported experimental results demonstrate the effectiveness of the proposed co-ranking scheme for image retrieval applications. In future work, the complexity of the proposed co-ranking scheme should be investigated and compared with other techniques.

References

1. Hirata, K., Kato, T.: Query by visual example - content-based image retrieval. In: Pirotte, A., Delobel, C., Gottlob, G. (eds.) EDBT 1992. LNCS, vol. 580, pp. 56–71. Springer, Heidelberg (1992)
2. Mumford, D.: Mathematical theories of shape: Do they model perception? In: Proceedings of SPIE Conference on Geometric Methods in Computer Vision, San Diego, California, vol. 1570, pp. 2–10 (1991)
3. Biederman, I.: Recognition-by-components: a theory of human image understanding. Psychological Review 94, 115–147 (1987)
4. Schomaker, L., Leau, E.D., Vuurpijl, L.: Using Pen-Based Outlines for Object-Based Annotation and Image-Based Queries. Visual Information and Information Systems, 585–592 (1999)
5. Wang, Z., Chi, Z., Feng, D.: Shape based leaf image retrieval. In: IEE Proceedings, Vision Image and Signal Processing, vol. 150, pp. 34–43 (2003)
6. Celebi, M.E., Aslandogan, Y.A.: A Comparative Study of Three Moment-Based Shape Descriptors. In: ITCC'05. International Conference on Information Technology: Coding and Computing, pp. 788–793 (2005)
7. Hu, M.: Visual Pattern Recognition by Moment Invariants. IRE Transactions on Information Theory 8, 179–187 (1962)
8. Teague, M.: Image analysis via the general theory of moments. Journal of the Optical Society of America 70, 920–930 (1980)
9. Khotanzad, A.: Invariant Image Recognition by Zernike Moments. IEEE Transactions on Pattern Analysis and Machine Intelligence 12, 489–497 (1990)
10. Belkasim, S.O., Shridhar, M., Ahmadi, M.: Pattern Recognition with Moment Invariants: A Comparative Study and New Results. Pattern Recognition 24, 1117–1138 (1991)
11. Mokhtarian, F., Bober, M.: Curvature scale space representation: Theory application and MPEG-7 standardization. Kluwer Academic Publishers, Boston (2003)
12. Wallace, T.P., Wintz, P A: An efficient three dimensional aircraft recognition algorithm using normalized Fourier descriptors. Computer Graphics and Image Processing 13, 99–126 (1991)
13. Abbasi, S., Mokhtarian, F., Kittler, J.: Curvature Scale Space Image in Shape Similarity Retrieval. Multimedia Systems 7, 467–476 (1999)
14. Chauang, G., Kuo, C.: Wavelet descriptor of planar curves: Theory and applications. IEEE Transaction on Image Processing 5, 56–70 (1996)
15. Adamek, T., O'Connor, N.E.: A Multiscale Representation Method for Nonrigid Shapes with a Single Closed Contour. IEEE Transactions on Pattern Analysis and Machine Intelligence 14, 742–753 (1996)
16. Zhang, D.S., Lu, G.: Study and Evaluation of Different Fourier Methods for Image Retrieval. International Journal of Computer Vision 23, 33–49 (1996)
17. Kim, W., Kim, Y.: A region-based shape descriptor using Zernike moments. Signal Processing: Image Communication 16, 95–102 (1996)
18. El Rube, I., Alajlan, N., Kamel, M.S., Ahmed, M., Freeman, G.: Efficient Multiscale Shape-Based Representation and Retrieval. In: Kamel, M., Campilho, A. (eds.) ICIAR 2005. LNCS, vol. 3656, pp. 415–422. Springer, Heidelberg (2005)